

Generative Scenario Rollouts for End-to-End Autonomous Driving

Rajeev Yasarla¹, Deepti Hegde¹, Shizhong Han¹, Hsin-Pai Cheng¹, Yunxiao Shi¹, Meysam Sadeghigooghari², Shweta Mahajan^{1†}, Apratim Bhattacharyya¹, Litian Liu¹, Risheek Garrepalli¹, Thomas Svantesson², Fatih Porikli¹, Hong Cai¹

¹ Qualcomm AI Research* ² Qualcomm Technologies, Inc.

Abstract

Vision-Language-Action (VLA) models are emerging as highly effective planning models for end-to-end autonomous driving systems. However, current works mostly rely on imitation learning from sparse trajectory annotations and under-utilize their potential as generative models. We propose Generative Scenario Rollouts (GeRo), a plug-and-play framework for VLA models that jointly performs planning and generation of language-grounded future traffic scenes through an autoregressive rollout strategy. First, a VLA model is trained to encode ego vehicle and agent dynamics into latent tokens under supervision from planning, motion, and language tasks, facilitating text-aligned generation. Next, GeRo performs language-conditioned autoregressive generation. Given multi-view images, a scenario description, and ego-action questions, it generates future latent tokens and textual responses to guide long-horizon rollouts. A rollout-consistency loss stabilizes predictions using ground truth or pseudo-labels, mitigating drift and preserving text-action alignment. This design enables GeRo to perform temporally consistent, language-grounded rollouts that support long-horizon reasoning and multi-agent planning. On Bench2Drive, GeRo improves driving score and success rate by +15.7 and +26.2, respectively. By integrating reinforcement learning with generative rollouts, GeRo achieves state-of-the-art closed-loop and open-loop performance, demonstrating strong zero-shot robustness. These results highlight the promise of generative, language-conditioned reasoning as a foundation for safer and more interpretable end-to-end autonomous driving.

1. Introduction

Autonomous driving systems require robust navigation and planning capabilities in complex and dynamic environments. Recent approaches train end-to-end motion plan-

*Qualcomm AI Research is an initiative of Qualcomm Technologies, Inc.

†Work was completed while employed at Qualcomm AI Research.

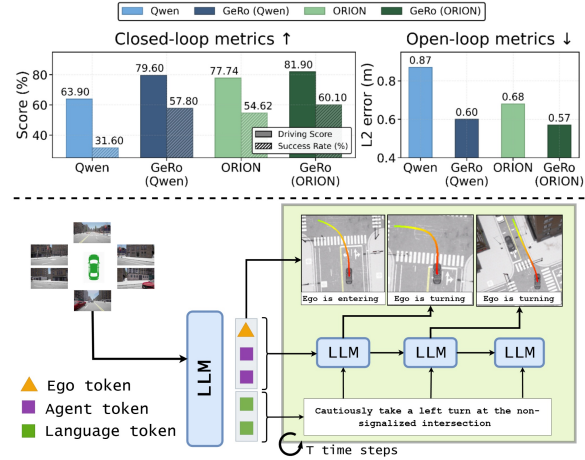


Figure 1. (Top) Closed-loop metrics (Driving Score and Success Rate) and open-loop metric (Trajectory L2 error) for different models. GeRo consistently improves both closed-loop and open-loop performance across baselines like Qwen2.5VL [3] and ORION [10]. (Bottom) GeRo scenario rollout pipeline: given a scenario description and multi-view observations, GeRo generates temporally consistent agent behaviors using a large language model (LLM) across time steps.

ners that map raw sensor inputs to future ego-vehicle trajectories [14, 21, 37, 43, 48]. Within this paradigm, Vision-Language-Action (VLA) models use large language models (LLMs) to integrate linguistic context into motion planning, enabling language-informed driving decisions [5, 9, 10, 33, 33, 39, 41, 50].

Despite this progress, current VLA models exhibit critical limitations and leave several directions underexplored.

- (1) Sparse language-action supervision: Driving datasets [10, 32, 35] often provide scene-level descriptions and Q&A pairs but rarely include fine-grained actions tied to temporal phases of driving events, making models brittle in ambiguous or long-tail scenarios, such as distinguishing overtaking from merging or localizing the ego vehicle’s intent within multi-step maneuvers [10].
- (2) Underutilized generative capability: Existing VLA methods rely

only on ground-truth trajectories for planning, overlooking the potential of autoregressive generation for scenario-level reasoning and exploration. (3) Descriptive vs. procedural language: Current language supervision typically describes what is happening rather than how actions unfold, limiting the model’s ability to capture procedural nuances necessary for planning and execution. (4) Language-action misalignment: Many datasets generate instruction–action pairs after collecting expert driving data [33], so models often infer from visual cues only and ignore language, causing failures like “stop for red light” paired with acceleration.

To address these issues, we propose Generative Scenario Rollouts (GeRo), a plug-and-play training framework that unifies VLA models with scenario generation for language-aligned action prediction and improved planning robustness. To the best of our knowledge, this is the first work to jointly perform scenario generation with motion prediction, planning, and visual question-answering. GeRo has two phases:

- **Pretraining:** In this stage, the VLA model is trained to encode ego and agent dynamics into a compact shared token space. The model is jointly supervised for planning, multi-agent motion prediction with auxiliary bounding-box cues, and visual question answering. This stage is crucial for binding linguistic and behavioral representations, enabling text-aligned generation beyond paired annotations, thus reducing language-action misalignment.
- **Language-conditioned Scenario Rollout:** In this phase, the model autoregressively predicts future latent tokens and ego-aligned action descriptions based on past latent tokens. The tokens are fed back to the VLA model to guide long-horizon reasoning. Predictions are stabilized using a consistency loss that mitigates drift and enforces text-action consistency. Specifically, we enforce temporal consistency by aligning the latent distribution of rollout predictions with the pretrained latent distribution for future time steps using KL-Divergence. When ground-truth data is available, imitation learning is applied by supervising the model with corresponding waypoints and motion trajectories to enforce scenario generation. However, relying solely on imitation learning can lead to suboptimal performance; therefore, we introduce reinforcement learning based feedback with GRPO [34] for the scenario rollouts. This incorporates rewards relating to collision avoidance, time-to-collision (TTC), and language-aligned scenario generation using question–answer pairs relating to the action of the ego-vehicle.

Our contributions are threefold:

1. We introduce **GeRo**, a generative scenario rollout framework that integrates autoregressive scenario generation into VLA models. This design couples temporal reasoning with linguistic context, enabling scenario rollouts that predict future motions of traffic agents and ego ac-

tions for robust planning.

2. We propose a novel set of reward functions for GRPO-based reinforcement learning that jointly optimize trajectory accuracy and semantic alignment with language descriptions during scenario rollouts. These rewards incorporate safety-critical metrics such as collision avoidance and time-to-collision, ensuring high-fidelity and interpretable planning behavior.
3. **GeRo** introduces an interactive Visual Question Answering (VQA) component that grounds ego-vehicle intent in natural language, allowing the model to answer scenario-specific questions during rollouts. This enhances interpretability and provides a mechanism for language-guided reasoning in complex driving environments.

Through extensive closed-loop and open-loop experiments on Bench2Drive, we show that GeRo significantly outperforms VLA baselines [10] and other end-to-end motion planners [14, 20, 21], particularly in corner cases and zero-shot planning, highlighting the importance of scenario-level reasoning and language-action alignment for end-to-end autonomous driving.

2. Related Works

2.1. VLA for Autonomous Driving

While conventional models like VAD [21] and UniAD [14] offer fast inference and streamlined integration of perception, prediction, and planning, they often struggle with generalization in long-tail scenarios. Recent LLM-based approaches [5, 7, 9, 10, 33, 33, 39–41, 50] integrate world-model reasoning with language, improving robustness in long-tail scenarios. GPT-Driver [29] reformulates planning as text generation, converting observations into language prompts and leveraging chain-of-thought reasoning [42]. EMMA [16], trained on large-scale driving datasets, enables models like Gemini [5] to predict discrete textual plans with strong open-loop performance. Hybrid dual-system architectures combine fast end-to-end models with slower, reasoning-capable VLMs. DriveVLM [39] employs a dual system where a VLM predicts low-frequency trajectories refined by a conventional planner, while Senna [9] introduces meta-actions to guide VAD for semantically aligned motion trajectories. ORION [10] proposes a unified end-to-end framework that aligns VLM reasoning with trajectory prediction for close-loop scenarios. SimLingo [33] further improves language–scene alignment, achieving competitive accuracy on Bench2Drive, leveraging additional, higher-quality training data.

2.2. Driving Scenario Generation

Generative models, particularly diffusion-based architectures, have shown promise in modeling the stochastic nature of driving behavior and generating diverse, multimodal

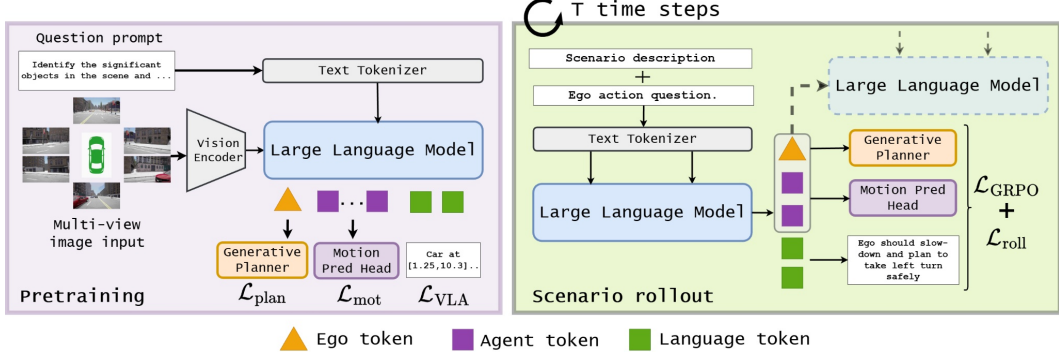


Figure 2. **An overview of GeRo’s two stage framework.** Left: GeRo pretraining stage of the Vision–Language–Action (VLA) model. Multi-view images and scenario prompts are encoded into visual and text tokens and projected by the LLM head to compute ego and agent tokens. These tokens drive are passed to the *generative planner* and the *motion prediction head*. The planning, motion and language prediction tasks are supervised by their respective loss functions($\mathcal{L}_{\text{plan}}$, \mathcal{L}_{mot} , \mathcal{L}_{VLA}). . Right: GeRo’s autoregressive rollout stage. Given a scenario description and ego-action questions, GeRo performs scenario rollout to predict future tokens for T steps, decoding them into ego waypoints, multi-agent trajectories, and language outputs. Rollouts are optimized with consistency loss ($\mathcal{L}_{\text{roll}}$) and reinforcement feedback ($\mathcal{L}_{\text{GRPO}}$) for robust scenario grounding.

trajectories. DiffusionDrive [25] introduces a truncated diffusion process with anchor priors, enabling real-time multi-modal planning. GoalFlow [45] applies goal-point guidance with flow matching for high-quality trajectory generation, while DiffusionPlanner [49] redefines planning as future trajectory generation, jointly producing plans and motion forecasts. InfGen proposed to do the arbitrary resolution image generation in the latent space with diffusion models [12]. In the VLA context, ORION extends its framework with a VAE-based generative planner that translates LLM outputs into trajectory distributions [10]. DiVLA [28] combines autoregressive reasoning with diffusion policy learning, introducing a reasoning injection module that enhances interpretability and generalization. These generative VLA models establish a foundation for explainable, multimodal driving policies, motivating our generative rollout approach.

2.3. Reinforcement Learning for Driving

Reinforcement learning (RL) has emerged as a powerful paradigm for improving policy generalization and robustness in autonomous driving. Unlike imitation learning, which suffers from covariate shift [31], RL enables agents to learn from interaction and adapt to novel scenarios. RAD [11] trains end-to-end agents in photorealistic 3DGS environments, demonstrating improved generalization. CarPlanner [47] introduces an autoregressive policy that generates consistent multimodal trajectories, outperforming imitation-based baselines through expert-guided reward shaping. Recent efforts also explore synergy between RL and VLMs: GenDrive [15] combines diffusion models with RL and reward modeling, while AlphaDrive [23], R2SE [27], and TrajHF [24] incorporate GRPO-based training to enhance policy stability and generalization. By integrating VLMs into the RL loop, these approaches enable semantic grounding and improve decision-

making in complex, long-tail scenarios.

3. Methodology

We present GeRo, a generative scenario rollout framework for VLA models that unifies planning and autoregressive scenario generation. GeRo is shown in Figure 2. In GeRo, rollout operates in a token space that is learned in a pre-training stage, where ego and agent states are represented as compact latent tokens. Given latent ego-tokens and agent tokens along with a high-level scenario description and a question regarding the actions of the ego-vehicle, the GeRo framework uses a VLA model to autoregressively generate future scenarios by predicting their latent ego and agent tokens. The model is also jointly trained to perform planning, motion prediction, and visual question-answering. These tasks are supervised under GRPO [34] with a series of specially designed reward functions. An overview of the rollout mechanism can be seen in Figure 3.

3.1. Problem Formulation

Consider a driving scene at time t consisting of an ego vehicle and a set of N_t traffic participants \mathcal{A}_t . Given a sequence of multi-view images, a scene description, and information about the state of the ego-vehicle x_t^e and the state of the other traffic participants $x_t^{(a_i)}$, the objective of GeRo is to jointly predict (i) an ego trajectory $\hat{\tau}_t^e$ that supports safe and efficient driving, (ii) future motions of surrounding agents $\{\hat{\tau}_t^{(a_i)}\}_{i=1}^{N_t}$ ¹, and (iii) a scenario-based ego-action answer to question q . The ego state comprises of pose, velocity, and acceleration. The state of agent a_i consists of the agent’s

¹For notational simplicity, we drop the agent indices when appropriate. For example, we refer to $\{\hat{\tau}_t^{(a_i)}\}_{i=1}^{N_t}$ as $\{\hat{\tau}_t^{(a_i)}\}$, and we refer the set of ego and agent trajectories, $\{\hat{\tau}^e, \{\hat{\tau}_t^{(a_i)}\}_{i=1}^{N_t}\}$ as $\{\hat{\tau}_t\}$, when it is clear from the context.

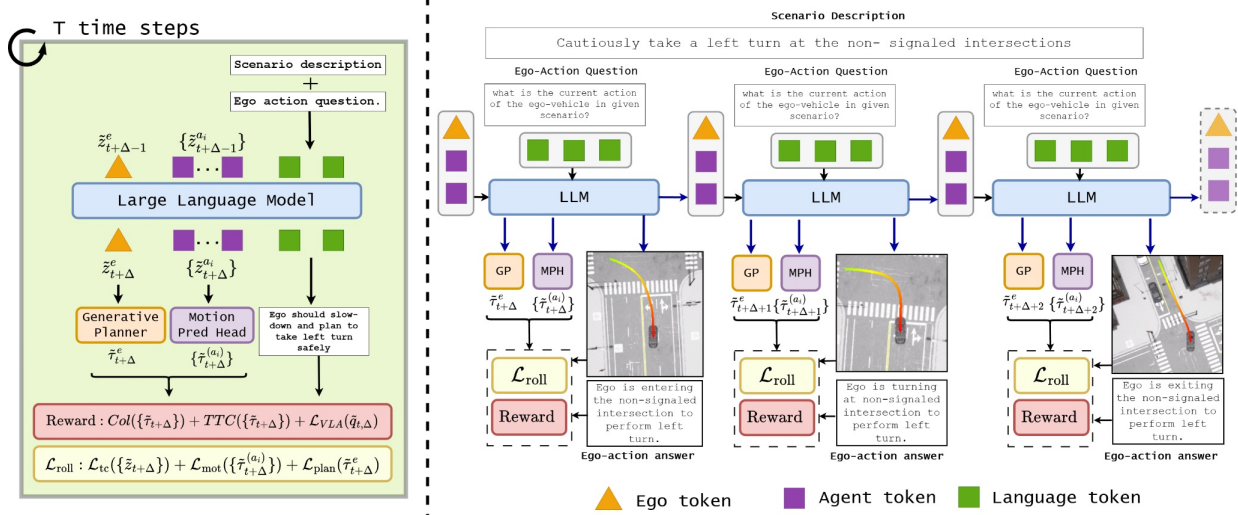


Figure 3. **Autoregressive scenario rollout in GeRo.** At time t , GeRo consumes ego and agent tokens along with scenario description and ego-action questions, and predicts next-step tokens using the LLM head. These tokens are decoded into ego trajectories, multi-agent trajectories, and language answers. The process repeats for T steps, with updated scenario descriptions and ego-action questions at rollout each step, enabling consistent rollouts aligned with text and environment dynamics. Rollouts are optimized using the consistency loss $\mathcal{L}_{\text{roll}}$ and the reinforcement feedback loss $\mathcal{L}_{\text{GRPO}}$ for robust planning and reasoning.

class, bounding box, motion trajectory, velocity, and acceleration.

3.2. Architecture

GeRo provides a general plug-and-play framework for Vision-Language-Action models. The architecture thus follows several recent end-to-end planners that leverage multi-modal large language models for motion planning [10, 38, 41]. The vision encoder and the text tokenizer project image and text inputs to a common token embedding space. The central component is the large language model (LLM), which projects multi-modal tokens into a series of compact latent representations of the ego-vehicle and the surrounding agents. The LLM also predicts a scene description and answers questions related to the ego-vehicle behavior. Lastly, the framework contains a variational autoencoder (VAE) planning head and a motion prediction head.

3.3. Pretraining

The objective of the pretraining stage is to achieve a good initialization of action tokens for stable scenario generation in the token space. To this end, we first pretrain the VLA model to learn a compact tokenization of ego and agent dynamics. In this stage, we supervise three heads: (i) a planning head, which predicts future ego trajectory, (ii) the motion head, which predicts future multi-agent trajectories, and (iii) the large language model, which is trained to predict scene descriptions and perform visual question answering. The model is also trained to predict the detection bounding box of the agents along with their corresponding trajectories, $\{\hat{\tau}_t^{(a_i)}, \hat{\phi}_t^{(a_i)}\}_{i=1}^{N_t}$ to accelerate convergence of

trajectory prediction in the motion head. This pretraining stage teaches the model to encode and decode latent tokens for both ego and agents that remain consistent and representative of the scenario.

Pretraining loss functions The planning head is supervised by using two losses: an L1 loss for waypoint regression and a collision loss. The motion prediction head is supervised using (i) focal loss [26] for classification of agent types, (ii) L1 loss for trajectory prediction, and (iii) L1 loss for 3D bounding box detection. The LLM is trained with a cross-entropy loss for language prediction, following [3]. Let $\mathcal{L}_{\text{plan}}$, \mathcal{L}_{mot} , and \mathcal{L}_{VLA} denote these respective terms; the overall pretraining loss is defined as

$$\mathcal{L}_{\text{pre}} = \mathcal{L}_{\text{plan}} + \mathcal{L}_{\text{mot}} + \mathcal{L}_{\text{VLA}}. \quad (1)$$

3.4. Generative Scenario Rollout

Scenario rollout. Given a sequence of multi-view images up to time t , GeRo first computes the latent ego token z_t^e , the latent agent tokens $\{z_t^{(a_i)}\}$, and scenario description s_t , as shown in Figure 2. Next, GeRo performs autoregressive rollouts in the token space for T total steps as shown in Figure 3. Conditioned on latent tokens $\{z_t\}$, multi-view images at time t , a scenario description s , and the ego-action question $q_{t,1} \in Q$, the generator predicts the next-step tokens $\{\tilde{z}_{t+1}\}$ and the responses to the ego-action questions. These tokens are decoded into the ego trajectory, agent motion trajectories, and language outputs. The predicted tokens are fed back to the model along with a scenario description s and the next ego-action question $q_{t,\Delta+1}$, where

$\Delta \in [0, T - 1]$. This enables the model to generate the subsequent tokens $\{\tilde{z}_{t+\Delta+1}\}$, resulting in a rollout from t to $t + T$.

Language supervision A central goal of GeRo is to generate scenario rollouts of action tokens while grounding them in language, enabling the model not only to produce semantically coherent sequences of future tokens but also to reason about the context. Rollout is guided by a scene description s provided by the LLM and a question q relating to the action of the ego vehicle. Given each image sequence up to time t , its high-level scenario category, critical object information, and language annotations, the LLM is trained to then generate a rich scenario description s and corresponding ego-action questions Q that serve as language guidance for the autoregressive rollout.

Enforcing rollout consistency During scenario rollout, temporal consistency is enforced through two complementary mechanisms. First, the latent distribution of rollout predictions are aligned with the pretrained latent distribution for future time steps using KL-Divergence. Second, the model is supervised using imitation learning when ground truth labels are available.

When ground truth trajectory labels are unavailable, they can be constructed from latent tokens $z_{t+\Delta}$ predicted by the pretrained VLA model and conditioned on the input image sequence with additional future frames. This setup promotes temporal consistency across extended rollouts and helps mitigate compounding errors commonly observed in autoregressive generation.

To stabilize training over long horizons, we apply step-wise temporal consistency supervision \mathcal{L}_{tc} using pretraining heads under two regimes:

- **Ground-Truth Supervision:** When ground-truth data is available, we supervise the model using true states $\{x_{t+\Delta}\}$ and trajectories $\{\tau_{t+\Delta}\}$, providing accurate targets for each rollout step.
- **Model-Based Supervision:** In the absence of ground-truth, we rely on tokens $\{z_{t+\Delta}\}$ predicted by the pretrained VLA model (refer section 3.3) using corresponding input image sequence as reference targets. These predictions serve as pseudo-labels to guide GeRo during unsupervised rollout steps. The token-consistency loss is defined as: $\mathcal{L}_{tc}(\{\tilde{z}_{t+\Delta}\}) = \text{KL}(\{\tilde{z}_{t+\Delta}\} \parallel \{z_{t+\Delta}\})$, where $\text{KL}(\cdot \parallel \cdot)$ denotes the Kullback–Leibler divergence. This formulation enforces temporal consistency in scenario generation by alignment between the rollout predictions and the latent distribution of the pre-trained model.

This rollout consistency loss encourages alignment between the predicted and reference sequences—whether derived from ground-truth or VLA-generated pseudo-labels—thereby reducing drift and improving the fidelity of long-horizon planning. The rollout loss is formulated by integrating both planning and motion prediction components

as follows:

$$\mathcal{L}_{\text{roll}} = \sum_{\Delta=1}^T \left[\mathcal{L}_{tc}(\{\tilde{z}_{t+\Delta}\}) + \mathcal{L}_{\text{plan}}(\{\tilde{\tau}_{t+\Delta}\}) + \mathcal{L}_{\text{mot}}(\{\tilde{\tau}_{t+\Delta}\}) \right] \quad (2)$$

RL with GRPO Feedback Scenario rollout can result in a wide range of environmental dynamics and ego-agent interaction patterns. Consequently, GeRo rollouts often exhibit multi-modal behavior. Relying solely on imitation-based optimization, as defined in Eq. 2, may lead to sub-optimal outcomes [30], and is insufficient to address distributional shifts, long-tail events, and novel scenarios encountered in real-world driving. To mitigate these challenges and ensure safe, high-fidelity rollout generation, we introduce an on-policy Reinforcement Learning (RL) fine-tuning stage using Generalized Rollout Policy Optimization (GRPO) [34]. During rollout, we compute differentiable surrogate rewards that capture safety-critical metrics, including:

- **Collision Loss:** Penalizes predicted trajectories that result in collisions.
- **Time-to-Collision (TTC) Penalty:** Encourages longer TTC to promote safer interactions.
- **Language prediction accuracy (\mathcal{L}_{VLA}):** computes the cross-entropy loss that measures semantic alignment between generated language outputs and reference descriptions.

This reward formulation aligns policy optimization with both physical safety and semantic correctness. Empirically, this RL post-training significantly improves rollout quality. At each rollout step, the surrogate reward is computed as:

$$\mathbf{R}_{t+\Delta} = -\text{Coll}(\{\tilde{\tau}_{t+\Delta}\}) - \text{TTC}^{-1}(\{\tilde{\tau}_{t+\Delta}\}) - \mathcal{L}_{VLA}(\tilde{q}_{t+\Delta}), \quad (3)$$

where $\text{Coll}(\cdot)$ computes the collision rate, and $\text{TTC}(\cdot)$ measures the time-to-collision for the predicted trajectories $\{\tilde{\tau}_{t+\Delta}\}$. The GRPO algorithm aggregates step-wise advantages to update the generator over time. The advantage at each step is computed as: $\mathbf{A}_{t+\Delta} = \mathbf{R}_{t+\Delta} - b_{t+\Delta}$, where $b_{t+\Delta}$ is a baseline reward (is a learned value function). The reinforcement learning loss is then defined as:

$$\mathcal{L}_{\text{GRPO}} = -\mathbb{E} \left[\sum_{\Delta=1}^T \mathbf{A}_{t+\Delta} \right], \quad (4)$$

which encourages the model to favor actions that yield higher-than-average rewards across rollout steps.

3.5. Overall Supervision

The loss functions used in the two stages of GeRo are thus:

Table 1. Comparison of closed-loop and open-loop performance of end-to-end autonomous driving methods on the Bench2Drive base set. Avg. L2 denotes the average trajectory error over 2 seconds at 2 Hz, following UniAD [14]. Abbreviations: NC = Navigation Command, TP = Target Point, DS = Driving Score, SR = Success Rate, M = Map, B = Bounding boxes, D = Depth, Mo = Motion prediction, O = Occupancy, S = Segmentation, E = Expert distillation.

Method	Reference	Condition	Aux. Sup.	Closed-loop Metric				Open-loop Metric
				DS↑	SR(%)↑	Efficiency↑	Comfortness↑	
TCP-traj [44]	NeurIPS 22	TP	E+Speed	59.90	30.00	76.54	18.08	1.70
TCP-traj w/o distillation [44]	NeurIPS 22	TP	Speed	49.30	20.45	78.78	22.96	1.96
ThinkTwice [18]	CVPR 23	TP	E+D+S+M	62.44	31.23	69.33	16.22	0.95
DriveAdapter [17]	ICCV 23	TP	E+S	64.22	33.08	70.22	16.01	1.01
AD-MLP [46]	arXiv 23	NC	None	18.05	0.00	48.45	22.63	3.64
UniAD-Tiny [14]	CVPR 23	NC	M+B+Mo+O	40.73	13.18	123.92	47.04	0.80
UniAD-Base [14]	CVPR 23	NC	M+B+Mo+O	45.81	16.36	129.21	43.58	0.73
VAD [21]	ICCV 23	NC	M+B+Mo	42.35	15.00	157.94	46.01	0.91
GenAD [48]	ECCV 24	NC	M+B+Mo	44.81	15.90	-	-	-
MoMAD [36]	CVPR25	NC	M+B+Mo	44.54	16.71	170.21	48.63	0.87
DriveTransformer-Large [20]	ICLR 25	NC	M+B+Mo	63.46	35.01	100.64	20.78	0.62
Qwen2.5VL [3]	arXiv 23	NC	B+Mo	63.90	31.60	119.34	10.11	0.87
ORION [10]	ICCV 25	NC	M+B+Mo	77.74	54.62	151.48	17.38	0.68
ORION (Qwen2.5VL) [10]	ICCV 25	NC	M+B+Mo	76.88	53.90	146.16	24.75	0.72
GeRo (Qwen2.5VL) (ours)	-	NC	B+Mo	79.60	57.80	159.66	44.75	0.60
GeRo (ORION) (ours)	-	NC	M+B+Mo	81.90	60.10	176.51	40.22	0.57

Table 2. Multi-ability performance Comparison for E2E-AD methods on Bench2Drive base set. NC = Navigation Command, TP = Target Point, M = Map, B = Bounding boxes, D = Depth, Mo = Motion prediction, O = Occupancy, S = Segmentation, E = Expert distillation.

Method	Reference	Condition	Aux. Sup.	Ability (%) ↑					
				Merging	Overtaking	Emergency Brake	Give Way	Traffic Sign	Mean
TCP-traj [44]	NeurIPS 22	TP	E+Speed	28.84	24.29	51.67	40	46.28	34.22
TCP-traj w/o distillation [44]	NeurIPS 22	TP	Speed	28.72	28.72	48.33	40	28.72	34.10
ThinkTwice [18]	CVPR 23	TP	E+D+S+M	27.38	18.42	35.82	50	54.23	37.17
DriveAdapter [17]	ICCV 23	TP	E+S	28.38	28.38	47.50	50	56.43	42.14
AD-MLP [46]	arXiv 23	NC	None	0.00	0	0	0	4.35	0.87
UniAD-Tiny [14]	CVPR 23	NC	M+B+Mo+O	8.89	9.33	20	20	15.43	14.73
UniAD-Base [14]	CVPR 23	NC	M+B+Mo+O	8.89	9.33	20	20	14.21	14.49
VAD [21]	ICCV 23	NC	M+B+Mo	11.43	11.43	18.64	20	19.15	18.07
DriveTransformer-Large [20]	ICLR 25	NC	M+B+Mo	17.57	35.00	48.36	40	52.10	38.60
Qwen2.5VL [3]	arXiv 25	NC	B+Mo	14.27	28.91	30.11	30	24.73	25.60
ORION [10]	ICCV 25	NC	M+B+Mo	25.00	71.11	78.33	30	69.15	54.72
GeRo (Qwen2.5VL) (ours)	-	NC	B+Mo	37.83	72.81	83.10	50	66.17	61.98
GeRo (ORION) (ours)	-	NC	M+B+Mo	40.06	78.24	87.32	50	76.83	66.49

- **Stage-1: Pretraining.** The VLA model is trained to learn a representative action token space under the pretraining objective: \mathcal{L}_{pre} , summarized in Eq. 1.
- **Stage-2: Scenario rollout generation.** The VLA is optimized under the rollout consistency and reinforcement learning objectives: $\mathcal{L} = \mathcal{L}_{\text{roll}} + \mathcal{L}_{\text{GRPO}}$, detailed in Eq. 2 and Eq. 4.

Here, $\mathcal{L}_{\text{roll}}$ enforces consistency across autoregressive rollout, while $\mathcal{L}_{\text{GRPO}}$ incorporates GRPO-based reinforcement feedback for robust scenario grounding.

4. Experimental setup

4.1. Dataset and Evaluation Metrics

Dataset. GeRo is trained and evaluated on the Bench2Drive [19] dataset, a closed-loop benchmark based on CARLA [6] for end-to-end autonomous driving. We use the official set of 1000 clips (950 for training, 50 for open-loop validation), each covering about 150

meters of driving in diverse traffic scenes. Closed-loop evaluation follows the official protocol on 220 routes across 44 interactive scenarios. For open-loop planning, we use the nuScenes [4] planning benchmark, which contains 28,000 samples in a 22k/6k training/validation split.

VQA Dataset. Language annotations for the scene description and visual question answering tasks are obtained from the ChatB2D [10] dataset in conjunction with Bench2Drive [19], and the DriveLM-nuScenes [35] dataset. We generate additional scenario descriptions and ego-action question-answer pairs for training GeRo during scenario generation rollout (more details in supplementary).

Metrics. Bench2Drive closed-loop metrics include Driving Score (DS), Success Rate (SR), Efficiency, Comfort, and Multi-Ability. DS combines route completion and violation penalties; SR measures successful completion; Efficiency and Comfort assess speed and smoothness. Multi-Ability evaluates five advanced urban driving skills.

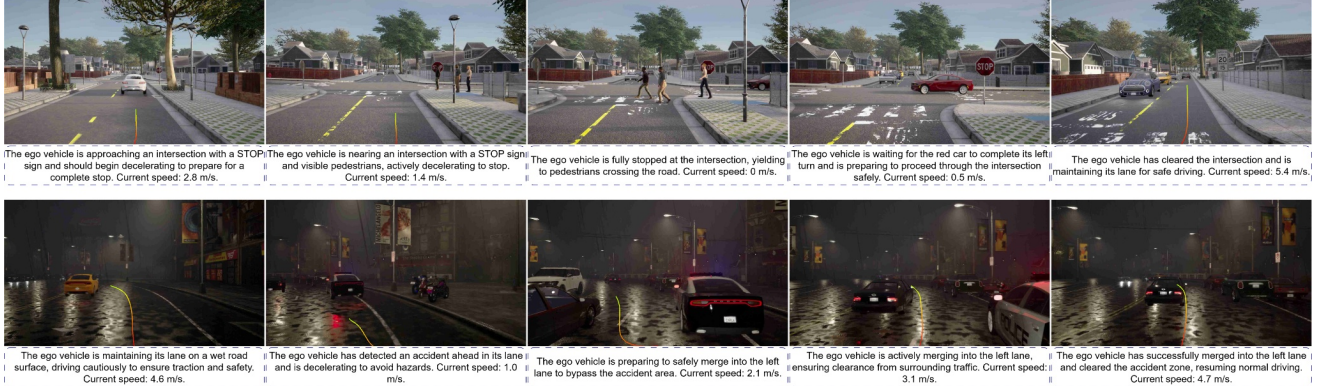


Figure 4. Qualitative examples of language-guided scenario rollouts using proposed GeRo on Bench2Drive. **Top:** Intersection scenarios with STOP signs and pedestrian interactions, where the ego vehicle demonstrates cautious deceleration, yielding, and safe left-turn. **Bottom:** Accident-handling scenarios under adverse weather, showing proactive hazard detection, lane-change planning, and smooth merging. Each frame includes generated textual reasoning aligned with the ego actions, highlighting temporal consistency and safety-aware decision.

Open-loop evaluation uses L2 trajectory error and collision rate, following ST-P3 [13].

4.2. Implementation Details

Model Architecture We implement the GeRo framework on two models. GeRo (Qwen) is built on the general multi-modal LLM Qwen2.5VL-3B [2] trained for end-to-end motion planning. GeRo (ORION) is built on the VLA model ORION [10]. In each case, GeRo leverages the vision encoder, text encoder, and the LLM of Qwen2.5VL. The vision encoder is the EVA-pretrained vision transformer (ViT) [8]. The motion prediction head is a stack of three MLP layers. The generative planning head is a variational autoencoder (VAE) from [10]. In GeRo (ORION), we utilize the auxiliary information and tasks used by the ORION model, while GeRo (Qwen) does not depend on HD maps. GeRo (Qwen) predicts trajectories conditioned only on the Navigation Command (NC), without explicit lane-center targets such as the Target Point (TP). GeRo (Qwen) also employs an anchor-free design, generating six trajectory modes aligned with those defined in Bench2Drive.

Training. All experiments are conducted on 8 NVIDIA H100 GPUs. GeRo is trained for 24 epochs in the first stage to learn robust token representations for latent tokens. In the second stage, GeRo is trained to autoregressively perform T scenario generation rollout steps (*i.e.* $t \rightarrow t+T$) and ground these predictions using the proposed losses for 24 epochs. We set $t = 4$ for all experiments, *i.e.*, a sequence of sets of four multi-view frames up to time t are passed to the VLA model. We set the rollout horizon $T = 8$ and, to increase temporal coverage, sample rollout steps at a uniform stride, *i.e.*, $\{t, t+r, \dots, t+rT\}$, where $r \in [1, 4]$, covering up to 32 future frames. In both training stages, all weights of Qwen2.5VL-3B are updated. We employ the AdamW optimizer with a cosine annealing learning rate scheduler, a weight decay of 0.01, and a learning rate of 2×10^{-4} .

5. Results and Discussion

We perform a thorough evaluation of GeRo in both closed-loop and open-loop planning settings. We demonstrate the capability of GeRo as a general plug-and-play framework for VLA models by implementing it on two end-to-end motion planners, Qwen2.5VL and ORION. We compare the performance of GeRo (Qwen) and GeRo (ORION) against recent end-to-end planners as well as the baselines: 1) The original ORION VLA model as proposed in [10], 2) ORION (Qwen2.5VL) which replaces the original Vicuna language model with that of Qwen2.5VL, and 3) Qwen2.5VL with added trajectory planning and motion prediction heads.

5.1. Closed-Loop Evaluation on Bench2Drive

Quantitative results Table 1 summarizes the quantitative closed-loop performance comparisons on 220 Bench2Drive test routes. GeRo achieves substantial gains over prior state-of-the-art methods. The baseline Qwen2.5VL model attains only 31.6% success rate and a driving score of 63.9, whereas GeRo (Qwen), equipped with guided scenario-generation rollouts and GRPO-based reinforcement learning, boosts performance to 79.6 driving score (+15.7) and 57.8% success rate (+26.2). Applying GeRo to ORION further improves this baseline, raising driving score from 77.74 to 81.90 (+4.16) and success rate from 54.62% to 60.10% (+5.5%). Notably, this model out-performs both baseline ORION models, which depend on HD map and bounding box annotations. A comparison of multi-ability performance is shown in Table 2. This table highlights similar trends: GeRo (Qwen) improves mean ability by 140% over the baseline Qwen2.5VL (*i.e.* 25.6 \rightarrow 61.98), while GeRo (ORION) delivers a 26.7% (*i.e.* 54.72 \rightarrow 66.49) improvement over ORION. Performance gains span critical skills such as merging, overtaking, emergency braking, yielding, and traffic-sign compliance—underscoring the effectiveness of language-guided scenario rollouts and rein-

Table 3. Comparison of E2E-AD methods on the nuScenes [4] validation set. \dagger indicates zero-shot testing trained on Bench2Drive and evaluated on nuScenes. Ego-status is not used in this experiment. Abbreviations: M = Map, B = Bounding boxes, D = Depth, Mo = Motion prediction, O = Occupancy.

Method	Aux. Sup.	L2 (\downarrow)				Collision Rate (\downarrow)			
		1s	2s	3s	Avg.	1s	2s	3s	Avg.
ST-P3 [13]	M+B+D	1.33	2.11	2.90	2.11	0.23	0.62	1.27	0.71
UniAD [14]	M+B+Mo+O	0.48	0.96	1.65	1.03	0.05	0.17	0.71	0.31
OccNet [1]	M+B+O	1.29	2.13	2.99	2.14	0.21	0.59	1.37	0.72
VAD-Base [21]	M+B+Mo	0.54	1.15	1.98	1.22	0.04	0.39	1.17	0.53
GenAD [48]	M+B+Mo	0.36	0.83	1.55	0.91	0.06	0.23	1.00	0.43
Senna [22]	M+B+Mo	0.37	0.54	0.86	0.59	0.09	0.12	0.33	0.18
Qwen2.5VL [3]	B+Mo	0.52	0.80	1.56	0.96	0.10	0.37	1.32	0.60
ORION [10]	M+B+Mo	0.43	0.64	1.01	0.69	0.09	0.29	0.94	0.44
GeRo (Qwen2.5VL) \dagger	B+Mo	0.24	0.41	0.70	0.45	0.11	0.22	0.42	0.25
GeRo (Qwen2.5VL)	B+Mo	0.16	0.27	0.50	0.31	0.06	0.10	0.26	0.14
GeRo (ORION) \dagger	M+B+Mo	0.16	0.32	0.61	0.36	0.08	0.16	0.39	0.21
GeRo (ORION)	M+B+Mo	0.12	0.24	0.46	0.27	0.05	0.09	0.22	0.12

Table 4. Ablation study of GeRo (Qwen) on Bench2Drive. The baseline model is Qwen2.5VL-3B. We report Driving Score (DS) and Success Rate (SR). Q : ego-action question–answer pairs, Sc Desc: scenario descriptions, tc: temporal consistency.

ID	Sc Desc	Q	Pretraining			Scenario Generation Rollout				Closed-loop metric			
			$\mathcal{L}_{\text{plan}}$			$\mathcal{L}_{\text{roll}}$				DS	SR		
			$\mathcal{L}_{\text{plan}}$	\mathcal{L}_{mot}	\mathcal{L}_{VQA}	$\mathcal{L}_{\text{roll}}$	$\mathcal{L}_{\text{plan}}$	\mathcal{L}_{mot}	Coll	TTC	\mathcal{L}_{VLA}		
1	x	x	\checkmark									58.2	27.4
2	x	x	\checkmark	\checkmark								61.1	28.2
3	\checkmark	x	\checkmark	\checkmark	\checkmark							63.9	31.6
4	\checkmark	x	\checkmark	\checkmark	\checkmark	\checkmark	\checkmark	\checkmark				67.8	40.1
5	\checkmark	x	\checkmark	\checkmark	\checkmark	\checkmark	\checkmark	\checkmark				69.2	46.6
6	\checkmark	x	\checkmark	\checkmark	\checkmark	\checkmark	\checkmark	\checkmark	\checkmark			74.4	50.4
7	\checkmark	x	\checkmark	\checkmark	\checkmark	\checkmark	\checkmark	\checkmark	\checkmark	\checkmark		76.9	54.4
8	\checkmark	x	\checkmark	\checkmark	\checkmark	\checkmark	\checkmark	\checkmark	\checkmark	\checkmark		78.5	55.7
9	\checkmark	\checkmark	\checkmark	\checkmark	\checkmark	\checkmark	\checkmark	\checkmark	\checkmark	\checkmark		79.6	57.8

forcement learning for robust action grounding.

Qualitative results Figure 4 illustrates GeRo’s language-conditioned rollouts in complex urban environments, encompassing challenges such as occlusions, pedestrian crossings, yielding interactions, and wet road conditions. The ego vehicle dynamically adapts its trajectory in response to evolving scene context—slowing near cross-walks, yielding to oncoming or turning vehicles, and proceeding only after potential conflicts have cleared. These behaviors align with the reasoning articulated in the generated ego-action responses, demonstrating a correspondence between textual intent and physical execution. This alignment underscores how scenario-grounded rollouts enable safe, context-aware planning.

5.2. Open-Loop Evaluation

We further evaluate open-loop trajectory prediction on the nuScenes and Bench2Drive planning benchmarks. This assesses both generalization and motion-forecasting quality. Our proposed GeRo delivers substantial gains over Qwen2.5VL and ORION baselines. In Table 1, GeRo shows a consistent drop in trajectory error across both baselines on Bench2Drive. Table 3 contains open-loop plan-

ning results on nuScenes. Compared to Qwen2.5VL, GeRo (Qwen) reduces L2 trajectory error from 0.96 to 0.31 (-67.7%) and collision rate from 0.60 to 0.14 (-76.7%). In the zero-shot setting, errors still drop to 0.45 (-53.1%) with collisions at 0.25 (-58.3%), highlighting strong cross-dataset generalization enabled by scenario-grounded rollouts. Using ORION as the backbone, GeRo (ORION) further improves L2 trajectory error from 0.69 to 0.27 (-60.9%) and collision rate from 0.44 to 0.12 (-72.7%). Zero-shot again shows notable gains (0.36, -47.8%; 0.21, -52.3%).

5.3. Ablation Study

Table 4 summarizes the ablation experiments of GeRo on the Bench2Drive dataset using Qwen2.5VL-3B as the baseline model. We report the closed-loop metrics Driving Score (DS) and Success Rate (SR).

Pretraining. IDs 1–3 in Table 4 show the impact of pre-training losses $\mathcal{L}_{\text{plan}}$, \mathcal{L}_{mot} , \mathcal{L}_{VLA} . Incorporating scenario descriptions and visual question answering (VQA) improves baseline performance, indicating that language grounding during pretraining enhances planning robustness.

Scenario rollout. IDs 4–6 evaluate the contributions of rollout-consistency losses $\mathcal{L}_{\text{roll}}$ within the proposed GeRo scenario generation framework. Even under model-based supervision—where ground truth is not required and we rely on predicted tokens $\{z_{t+1}\}$ from the pretrained VLA using $I_{1:t}$ as reference targets—computing \mathcal{L}_{tc} yields notable gains (+3.9 DS, +8.5% SR). Further incorporating ground-truth trajectories $\{\tau_{t+\Delta}\}$ for \mathcal{L}_{mot} and $\mathcal{L}_{\text{plan}}$ boosts performance by an additional +6.6 DS and +10.3% SR, demonstrating the value of accurate trajectory supervision during rollouts.

Reinforcement learning with GRPO. IDs 7–9 analyze the effect of GRPO-based reinforcement learning losses $\mathcal{L}_{\text{GRPO}}$. Using collision and time-to-collision (TTC) rewards during scenario rollouts improves DS by +4.1 and SR by +5.3%. Finally, introducing ego-action question–answer pairs Q (Figure 3) and leveraging the corresponding language alignment loss \mathcal{L}_{VLA} as an additional reward further enhances performance (+1.1 DS, +2.1% SR), highlighting the benefit of grounding ego intent in multi-step maneuvers through language-conditioned rollouts.

6. Conclusion

In this work, we introduced GeRo, a generative scenario rollout framework that unifies planning, multi-agent motion prediction, and scenario generation for robust end-to-end planning with Vision-Language-Action models. GeRo leverages shared latent tokenization and language-conditioned autoregressive rollout to enable temporally consistent and context-aware driving behavior. By integrating reinforcement learning with GRPO and aligning textual reasoning with action execution, our proposed GeRo

sets the new state-of-the-art performance with its robust, language-guided end-to-end planning. On standard autonomous driving benchmarks, GeRo provides significant improvements under both closed-loop and open-loop settings, as well as strong zero-shot sim-to-real generalization.

References

- [1] Awais Ahmed, Zeng Xiaoyang, Muhammad Hanif Tunio, Muhammad Hassan Butt, Syed Attique Shah, Yan Chengxiao, Farman Ali Pirzado, and Abdul Aziz. Occnet: Improving imbalanced multi-centred ovarian cancer subtype classification in whole slide images. In *2023 20th International Computer Conference on Wavelet Active Media Technology and Information Processing (ICCWAMTIP)*, pages 1–8. IEEE, 2023. 8
- [2] Jinze Bai, Shuai Bai, Shusheng Yang, Shijie Wang, Sinan Tan, Peng Wang, Junyang Lin, Chang Zhou, and Jingren Zhou. Qwen-vl: A versatile vision-language model for understanding, localization, text reading, and beyond. *arXiv preprint arXiv:2308.12966*, 2023. 7
- [3] Shuai Bai, Keqin Chen, Xuejing Liu, Jialin Wang, Wenbin Ge, Sibo Song, Kai Dang, Peng Wang, Shijie Wang, Jun Tang, Humen Zhong, Yuanzhi Zhu, Mingkun Yang, Zhao-hai Li, Jianqiang Wan, Pengfei Wang, Wei Ding, Zheren Fu, Yiheng Xu, Jiabo Ye, Xi Zhang, Tianbao Xie, Zesen Cheng, Hang Zhang, Zhibo Yang, Haiyang Xu, and Junyang Lin. Qwen2.5-vl technical report. *arXiv preprint arXiv:2502.13923*, 2025. 1, 4, 6, 8
- [4] Holger Caesar, Varun Bankiti, Alex H Lang, Sourabh Vora, Venice Erin Liang, Qiang Xu, Anush Krishnan, Yu Pan, Giancarlo Baldan, and Oscar Beijbom. nuscenes: A multi-modal dataset for autonomous driving. In *Proceedings of the IEEE/CVF conference on computer vision and pattern recognition*, pages 11621–11631, 2020. 6, 8
- [5] Long Chen, Oleg Sinavski, Jan Hünermann, Alice Karnsund, Andrew James Willmott, Danny Birch, Daniel Maund, and Jamie Shotton. Driving with llms: Fusing object-level vector modality for explainable autonomous driving. In *2024 IEEE International Conference on Robotics and Automation (ICRA)*, pages 14093–14100. IEEE, 2024. 1, 2
- [6] Alexey Dosovitskiy, German Ros, Felipe Codevilla, Antonio Lopez, and Vladlen Koltun. Carla: An open urban driving simulator. In *Conference on robot learning*, pages 1–16. PMLR, 2017. 6
- [7] Abhimanyu Dubey, Abhinav Jauhri, Abhinav Pandey, Abhishek Kadian, Ahmad Al-Dahle, Aiesha Letman, Akhil Mathur, Alan Schelten, Amy Yang, Angela Fan, et al. The llama 3 herd of models. *arXiv preprint arXiv:2407.21783*, 2024. 2
- [8] Yuxin Fang, Wen Wang, Binhui Xie, Quan Sun, Ledell Wu, Xinggang Wang, Tiejun Huang, Xinlong Wang, and Yue Cao. Eva: Exploring the limits of masked visual representation learning at scale. In *Proceedings of the IEEE/CVF conference on computer vision and pattern recognition*, pages 19358–19369, 2023. 7
- [9] Daocheng Fu, Xin Li, Licheng Wen, Min Dou, Pinlong Cai, Botian Shi, and Yu Qiao. Drive like a human: Rethinking autonomous driving with large language models. In *Proceedings of the IEEE/CVF Winter Conference on Applications of Computer Vision*, pages 910–919, 2024. 1, 2
- [10] Haoyu Fu, Diankun Zhang, Zongchuang Zhao, Jianfeng Cui, Dingkang Liang, Chong Zhang, Dingyuan Zhang, Hongwei Xie, Bing Wang, and Xiang Bai. Orion: A holistic end-to-end autonomous driving framework by vision-language instructed action generation. *arXiv preprint arXiv:2503.19755*, 2025. 1, 2, 3, 4, 6, 7, 8
- [11] Hao Gao, Shaoyu Chen, Bo Jiang, Bencheng Liao, Yiang Shi, Xiaoyang Guo, Yuechuan Pu, Haoran Yin, Xiangyu Li, Xinbang Zhang, et al. Rad: Training an end-to-end driving policy via large-scale 3dgs-based reinforcement learning. *arXiv preprint arXiv:2502.13144*, 2025. 3
- [12] Tao Han, Wanghan Xu, Junchao Gong, Xiaoyu Yue, Song Guo, Luping Zhou, and Lei Bai. Infgen: A resolution-agnostic paradigm for scalable image synthesis. In *Proceedings of the IEEE/CVF International Conference on Computer Vision*, pages 17941–17950, 2025. 3
- [13] Shengchao Hu, Li Chen, Penghao Wu, Hongyang Li, Junchi Yan, and Dacheng Tao. St-p3: End-to-end vision-based autonomous driving via spatial-temporal feature learning. In *European Conference on Computer Vision*, pages 533–549. Springer, 2022. 7, 8
- [14] Yihan Hu, Jiazhi Yang, Li Chen, Keyu Li, Chonghao Sima, Xizhou Zhu, Siqi Chai, Senyao Du, Tianwei Lin, Wenhui Wang, et al. Planning-oriented autonomous driving. In *Proceedings of the IEEE/CVF Conference on Computer Vision and Pattern Recognition*, pages 17853–17862, 2023. 1, 2, 6, 8
- [15] Zhiyu Huang, Xinshuo Weng, Maximilian Igl, Yuxiao Chen, Yulong Cao, Boris Ivanovic, Marco Pavone, and Chen Lv. Gen-drive: Enhancing diffusion generative driving policies with reward modeling and reinforcement learning fine-tuning. In *2025 IEEE International Conference on Robotics and Automation (ICRA)*, pages 3445–3451. IEEE, 2025. 3
- [16] Jyh-Jing Hwang, Runsheng Xu, Hubert Lin, Wei-Chih Hung, Jingwei Ji, Kristy Choi, Di Huang, Tong He, Paul Covington, Benjamin Sapp, Yin Zhou, James Guo, Dragomir Anguelov, and Mingxing Tan. Emma: End-to-end multimodal model for autonomous driving. *arXiv preprint arXiv:2410.23262*, 2024. 2
- [17] Xiaosong Jia, Yulu Gao, Li Chen, Junchi Yan, Patrick Langechuan Liu, and Hongyang Li. Driveadapter: Breaking the coupling barrier of perception and planning in end-to-end autonomous driving. In *ICCV*, 2023. 6
- [18] Xiaosong Jia, Penghao Wu, Li Chen, Jiangwei Xie, Conghui He, Junchi Yan, and Hongyang Li. Think twice before driving: Towards scalable decoders for end-to-end autonomous driving. In *CVPR*, 2023. 6
- [19] Xiaosong Jia, Zhenjie Yang, Qifeng Li, Zhiyuan Zhang, and Junchi Yan. Bench2drive: Towards multi-ability benchmarking of closed-loop end-to-end autonomous driving. In *NeurIPS 2024 Datasets and Benchmarks Track*, 2024. 6
- [20] Xiaosong Jia, Junqi You, Zhiyuan Zhang, and Junchi Yan. Drivetransformer: Unified transformer for scalable end-to-

end autonomous driving. In *The Thirteenth International Conference on Learning Representations*, 2025. 2, 6

[21] Bo Jiang, Shaoyu Chen, Qing Xu, Bencheng Liao, Jiajie Chen, Helong Zhou, Qian Zhang, Wenyu Liu, Chang Huang, and Xinggang Wang. Vad: Vectorized scene representation for efficient autonomous driving. In *Proceedings of the IEEE/CVF International Conference on Computer Vision*, pages 8340–8350, 2023. 1, 2, 6, 8

[22] Bo Jiang, Shaoyu Chen, Bencheng Liao, Xingyu Zhang, Wei Yin, Qian Zhang, Chang Huang, Wenyu Liu, and Xinggang Wang. Senna: Bridging large vision-language models and end-to-end autonomous driving. *arXiv preprint arXiv:2410.22313*, 2024. 8

[23] Bo Jiang, Shaoyu Chen, Qian Zhang, Wenyu Liu, and Xinggang Wang. Alphadrive: Unleashing the power of vlms in autonomous driving via reinforcement learning and reasoning. *arXiv preprint arXiv:2503.07608*, 2025. 3

[24] Derun Li, Jianwei Ren, Yue Wang, Xin Wen, Pengxiang Li, Leimeng Xu, Kun Zhan, Zhongpu Xia, Peng Jia, Xianpeng Lang, et al. Finetuning generative trajectory model with reinforcement learning from human feedback. *arXiv preprint arXiv:2503.10434*, 2025. 3

[25] Bencheng Liao, Shaoyu Chen, Haoran Yin, Bo Jiang, Cheng Wang, Sixu Yan, Xinbang Zhang, Xiangyu Li, Ying Zhang, Qian Zhang, et al. Diffusiondrive: Truncated diffusion model for end-to-end autonomous driving. In *Proceedings of the Computer Vision and Pattern Recognition Conference*, pages 12037–12047, 2025. 3

[26] Tsung-Yi Lin, Priya Goyal, Ross Girshick, Kaiming He, and Piotr Dollár. Focal loss for dense object detection. In *Proceedings of the IEEE international conference on computer vision*, pages 2980–2988, 2017. 4

[27] Haochen Liu, Tianyu Li, Haohan Yang, Li Chen, Caojun Wang, Ke Guo, Haochen Tian, Hongchen Li, Hongyang Li, and Chen Lv. Reinforced refinement with self-aware expansion for end-to-end autonomous driving. *arXiv preprint arXiv:2506.09800*, 2025. 3

[28] Jiaqi Liu, Peng Hang, Xiao Qi, Jianqiang Wang, and Jian Sun. Mtd-gpt: A multi-task decision-making gpt model for autonomous driving at unsignalized intersections. In *2023 IEEE 26th International Conference on Intelligent Transportation Systems (ITSC)*, pages 5154–5161. IEEE, 2023. 3

[29] Jiageng Mao, Yuxi Qian, Junjie Ye, Hang Zhao, and Yue Wang. Gpt-driver: Learning to drive with gpt. *arXiv preprint arXiv:2310.01415*, 2023. 2

[30] Takayuki Osa, Joni Pajarinen, Gerhard Neumann, J Andrew Bagnell, Pieter Abbeel, Jan Peters, et al. An algorithmic perspective on imitation learning. *Foundations and Trends® in Robotics*, 7(1-2):1–179, 2018. 5

[31] Youssef Al Ozaibi, Manolo Dulva Hina, and Amar Ramdane-Cherif. End-to-end autonomous driving in carla: A survey. In *IEEE Access*, pages 146866 – 146900. IEEE, 2024. 3

[32] Tianwen Qian, Jingjing Chen, Linhai Zhuo, Yang Jiao, and Yu-Gang Jiang. Nuscenes-qa: A multi-modal visual question answering benchmark for autonomous driving scenario. In *Proceedings of the AAAI Conference on Artificial Intelligence*, pages 4542–4550, 2024. 1

[33] Katrin Renz, Long Chen, Elahe Arani, and Oleg Sinavski. Simlingo: Vision-only closed-loop autonomous driving with language-action alignment. In *Proceedings of the Computer Vision and Pattern Recognition Conference*, pages 11993–12003, 2025. 1, 2

[34] Zhihong Shao, Peiyi Wang, Qihao Zhu, Runxin Xu, Junxiao Song, Xiao Bi, Huawei Zhang, Mingchuan Zhang, YK Li, Yang Wu, et al. Deepseekmath: Pushing the limits of mathematical reasoning in open language models. *arXiv preprint arXiv:2402.03300*, 2024. 2, 3, 5

[35] Chonghao Sima, Katrin Renz, Kashyap Chitta, Li Chen, Hanxue Zhang, Chengan Xie, Ping Luo, Andreas Geiger, and Hongyang Li. Drivelm: Driving with graph visual question answering. *arXiv preprint arXiv:2312.14150*, 2023. 1, 6

[36] Ziying Song, Caiyan Jia, Lin Liu, Hongyu Pan, Yongchang Zhang, Junming Wang, Xingyu Zhang, Shaoqing Xu, Lei Yang, and Yadan Luo. Don’t shake the wheel: Momentum-aware planning in end-to-end autonomous driving. In *Proceedings of the Computer Vision and Pattern Recognition Conference*, pages 22432–22441, 2025. 6

[37] Wenchao Sun, Xuewu Lin, Yining Shi, Chuang Zhang, Haoran Wu, and Sifa Zheng. Sparsedrive: End-to-end autonomous driving via sparse scene representation. *arXiv preprint arXiv:2405.19620*, 2024. 1

[38] Ran Tian, Boyi Li, Xinshuo Weng, Yuxiao Chen, Edward Schmerling, Yue Wang, Boris Ivanovic, and Marco Pavone. Tokenize the world into object-level knowledge to address long-tail events in autonomous driving. *arXiv preprint arXiv:2407.00959*, 2024. 4

[39] Xiaoyu Tian, Junru Gu, Bailin Li, Yicheng Liu, Chenxu Hu, Yang Wang, Kun Zhan, Peng Jia, Xianpeng Lang, and Hang Zhao. Drivevlm: The convergence of autonomous driving and large vision-language models. *arXiv preprint arXiv:2402.12289*, 2024. 1, 2

[40] Hugo Touvron, Thibaut Lavril, Gautier Izacard, Xavier Martinet, Marie-Anne Lachaux, Timothée Lacroix, Baptiste Rozière, Naman Goyal, Eric Hambro, Faisal Azhar, et al. Llama: Open and efficient foundation language models. *arXiv preprint arXiv:2302.13971*, 2023.

[41] Shihao Wang, Zhiding Yu, Xiaohui Jiang, Shiyi Lan, Min Shi, Nadine Chang, Jan Kautz, Ying Li, and Jose M Alvarez. Omnidrive: A holistic llm-agent framework for autonomous driving with 3d perception, reasoning and planning. *arXiv preprint arXiv:2405.01533*, 2024. 1, 2, 4

[42] Jason Wei, Xuezhi Wang, Dale Schuurmans, Maarten Bosma, Fei Xia, Ed Chi, Quoc V Le, Denny Zhou, et al. Chain-of-thought prompting elicits reasoning in large language models. *Advances in neural information processing systems*, 35:24824–24837, 2022. 2

[43] Xinshuo Weng, Boris Ivanovic, Yan Wang, Yue Wang, and Marco Pavone. Para-drive: Parallelized architecture for real-time autonomous driving. In *Proceedings of the IEEE/CVF Conference on Computer Vision and Pattern Recognition*, pages 15449–15458, 2024. 1

[44] Penghao Wu, Xiaosong Jia, Li Chen, Junchi Yan, Hongyang Li, and Yu Qiao. Trajectory-guided control prediction for

end-to-end autonomous driving: A simple yet strong baseline. *Advances in Neural Information Processing Systems*, 35:6119–6132, 2022. 6

[45] Zebin Xing, Xingyu Zhang, Yang Hu, Bo Jiang, Tong He, Qian Zhang, Xiaoxiao Long, and Wei Yin. Goalflow: Goal-driven flow matching for multimodal trajectories generation in end-to-end autonomous driving. In *Proceedings of the Computer Vision and Pattern Recognition Conference*, pages 1602–1611, 2025. 3

[46] Jiang-Tian Zhai, Ze Feng, Jinhao Du, Yongqiang Mao, Jiang-Jiang Liu, Zichang Tan, Yifu Zhang, Xiaoqing Ye, and Jingdong Wang. Rethinking the open-loop evaluation of end-to-end autonomous driving in nuscenes. *arXiv preprint arXiv:2305.10430*, 2023. 6

[47] Dongkun Zhang, Jiaming Liang, Ke Guo, Sha Lu, Qi Wang, Rong Xiong, Zhenwei Miao, and Yue Wang. Carplanner: Consistent auto-regressive trajectory planning for large-scale reinforcement learning in autonomous driving. In *Proceedings of the Computer Vision and Pattern Recognition Conference*, pages 17239–17248, 2025. 3

[48] Wenzhao Zheng, Ruiqi Song, Xianda Guo, Chenming Zhang, and Long Chen. Genad: Generative end-to-end autonomous driving. In *European Conference on Computer Vision*, pages 87–104. Springer, 2024. 1, 6, 8

[49] Yinan Zheng, Ruiming Liang, Kexin Zheng, Jinliang Zheng, Liyuan Mao, Jianxiong Li, Weihao Gu, Rui Ai, Shengbo Eben Li, Xianyuan Zhan, et al. Diffusion-based planning for autonomous driving with flexible guidance. *arXiv preprint arXiv:2501.15564*, 2025. 3

[50] Zewei Zhou, Tianhui Cai, Seth Z Zhao, Yun Zhang, Zhiyu Huang, Bolei Zhou, and Jiaqi Ma. Autovla: A vision-language-action model for end-to-end autonomous driving with adaptive reasoning and reinforcement fine-tuning. *arXiv preprint arXiv:2506.13757*, 2025. 1, 2